Biomechanical gait simulations with military body borne loads: An exploration of predicted gait kinematics, ground reaction forces & estimated metabolic cost of transport

T.A. van Kuijk
5160731

MSc Mechanical Engineering - BioMechanical Design
December 2023 - August 2024
Date of Defense: August 21st, 2024 10:45

Delft University of Technology
Faculty of Mechanical Engineering

Thesis committee
Dr. ir. A. Seth   TU Delft, Chair
Prof. dr. ir. J. Harlaar   TU Delft, Committee member
Dr. M.G.H. Wesseling   TU Delft, Committee member
MSc. B.J.C. Bastiaansen   TNO, Committee member

TUDelft

Commissioned by TNO

CONTENTS

ACRONYMS

- **2D** - Two dimensional
- **3D** - Three dimensional
- **CE** - Contractile element
- **CMA-ES** - Convariance matrix adaptation evolution strategy
- **CMC** - Computed muscle control
- **COM** - Centre of mass
- **COP** - Centre of pressure
- **DOF** - Degree of freedom
- **FVA** - Foot velocity algorithm
- **GRF** - Ground reaction force
- **HAT** - Head-arms-trunk
- **HS** - Heel strike
- **IMU** - Inertial measurement unit
- **m./mm.** - Muscolo/muscoli
- **mCoT** - Metabolic cost of transport
- **MS** - Mid-stance
- **MSK** - Musculoskeletal
- **MTU** - Muscle tendon unit
- **OCF** - Objective cost function
- **PT** - Physical training
- **RRA** - Reduce residual algorithm
- **RMSE** - Root-mean-square error
- **TO** - Toe-off

Biomechanical gait simulations with military body borne loads: An exploration of predicted gait kinematics, ground reaction forces & estimated metabolic cost of transport.

Abstract **– The ability to simulate the impact on performance of military body-borne loads enables effective analysis and optimisation of load and equipment configurations for military personnel performance. Additionally, these simulations can reduce research & development costs of new equipment by analysing its impact in an early stage of development. While research has been done into the effects of body borne loads on kinematics, ground reaction forces (GRF) and metabolic cost of transport, the accuracy and reliability of simulations are not clear yet.**
This study set out to predict loaded gait kinematics and GRFs and estimate metabolic cost of transport for gait at 1.5 m/s, carrying different types of military relevant body-borne loads, to evaluate the applied methods for implementation in a future load configuration optimisation tool.
The kinematic/GRF prediction was performed by forward dynamics simulations in SCONE/hyfydy, using a planar musculoskeletal model and a 2 gait-state controller, simulating 15 solutions for each load condition. While only 60% of experimentally measured differences between load conditions were correctly predicted, the expected differences from literature were all correctly predicted. It was assessed that improving the number of gait states and the number of optimisations per load condition is expected to improve these results. The metabolic cost of transport (mCoT) estimation was performed by the Computed Muscle Control algorithm of OpenSim, using experimental kinematics and ground reaction forces. However, small compounding errors in experimental data and data processing prevented accurate mCoT estimations. Although the applied kinematic/GRF and mCoT simulation methods could not be validated yet, based on these results, the study as a whole does show promise for the continued development of these models and their future implementation for loaded gait performance optimisation.
Index Terms—**Biomechanics, load carriage, kinematics, ground reaction forces, metabolic cost, predictive simulation, musculoskeletal modelling.**

INTRODUCTION

Carrying loads is essential to a variety of tasks of military personnel. These loads often consist of weapons, backpacks and personal protective equipment such as body armor and helmets. And while this equipment enables certain capabilities, the carried weight on the body also incurs negative effects during performed tasks. Increased risk of injury [1], reduced agility and mobility [2], reduced metabolic capacity and increased fatigue [3] all impact the performance in the field. Especially during military marching, the injury risk and reduced metabolic capacity are crucial, as marching often involves carrying large loads over a long duration [1].

However, not all carried locations of loads impact performance in the same way. For instance, research has shown that the metabolic effect of carrying a load of 15% body weight packed high in a backpack is comparable to carrying the same amount of mass distributed round the body Centre of Mass (COM), while carrying the same load packed low in the backpack incurs a significantly higher metabolic cost of transport (CoT) [4]. Likewise, carrying a load on the ankle has been shown to have approximately 2.5 times the metabolic effect of carrying that same load on the thigh, and about 6.5 times the effect of carrying it at the waist [5]. In addition to the metabolic cost of carrying loads, gait kinematics also change in different ways, dependant on the location of the load. An increase in forward trunk lean [6] and decrease in stride length [7] is observed when a mass is located low on the back, compared to that same mass high on the back. Conversely, the step length increases when mass is added to the foot but does not increase when the same mass is added to the thigh or waist [8]. These altered kinematics and kinetics increase the injury risk in load carriage tasks [1].

When evaluating possible equipment configurations for different tasks or purposes, it is important to understand the impact of the equipment on performance. Although it is theoretically possible to test every configuration of body-borne equipment for metabolic and kinematic impacts, it is not feasible due to extensive time and cost involved. Furthermore, when new equipment is still in the design phase, evaluating its contribution to the combined impact of

1

the equipment configuration, necessitates extensive and costly prototype testing. Using computational simulations to analyze the kinematic and metabolic effects of load carriage could drastically reduce testing time and expenses. By mitigating these constraints, the optimisation of load configuration becomes possible, thereby improving performance and enhancing capabilities of dismounted soldiers.

To simulate the impact of backpack loads, Dorn *et al* [9] previously used the biomechanical modelling software OpenSim [10] to predict gait kinematics and metabolic cost for four different load magnitudes. While their kinematic simulation showed promising results, their study had the major limitation that they were only able to simulate a single optimisation per load condition. This leaves the possibility that their optimisation result was a local optimisation minimum rather than the true (global) optimal solution. Recent advances in simulation software, such as the hyfydy plugin [11] for the SCONE predictive simulation software [12], and increased computational power have significantly reduced optimization times. This allows for multiple parallel optimizations, which can provide perspective on the quality of optimisation results and increases robustness of the methodology. Increasing the number of parallel simulations can therefore increase confidence in the results. As for the simulation of lower limb load carriage metabolic cost, recently Han *et al* [13] simulated muscle activation and metabolic cost for two added load magnitudes distributed over the leg. Their study had a limitation however, as the accuracy of muscle activation predictions was impacted by the lack of scaling of the musculoskeletal (MSK) model to match test subject anthropometry. This significantly reduced the accuracy of predicted muscle activation [14], not only compared to experimental EMG data but also the differences of muscle activation between load conditions. This is because different load conditions impact the activation of different muscles, according to their own study. The impact of not scaling the model, however, is not equal for all body segments, hence not equal for all muscles and thus not equal for load conditions.

The current study assesses the impact of loads carried on the trunk, similarly to Dorn *et al*, and the impact of loads carried on the lower limbs, similarly to Han *et al*, while addressing the mentioned limitations of both studies. This study will do so by increasing the number of parallel simulations for the prediction of kinematics and ground reaction forces (GRF), and use scaled models to match the anthropometry of test subjects in mCoT calculations, while assessing the impact of both trunk and lower limb loads. Furthermore, we will utilise a single experimental dataset of kinematics recorded by IMU based motion capture and force plate GRFs, both to validate the kinematic and GRF predictions done by the SCONE/hyfydy software and also as input for the metabolic modeling done by OpenSim. Using IMU based motion tracking for mCoT calculations in OpenSim has never been done to our knowledge. It is an alternative to the norm of optical marker tracking, but without the issues of marker occlusion experienced in motion capture with body borne loads [15].

The first goal set for this study is to use SCONE to simulate unloaded and loaded gait at military relevant marching pace of 1.5 m/s with leg and trunk loads, and evaluate whether the modeled differences between unloaded and loaded gait kinematics and GRF correspond those observed in experimental data. The second goal is to use OpenSim to generate a tracking simulation of IMU based kinematics and force plate GRF data to estimate mCoT for each load condition, and validate the simulated values against experimental indirect calorimetry data.

METHODS

To understand the impact of different types of body borne loads on kinematics, GRFs and mCoT, two different simulation strategies are applied. First, SCONE [12] with the hyfydy [11] plugin is used to predict gait kinematics and GRFs using a forward dynamics approach. Secondly, OpenSim [10] with an inverse kinematics approach is used to estimate the required muscle activation to achieve the input kinematics and GRFs. The input data required for this approach can also be used to validate the SCONE results and is gathered experimentally, as well as experimental mCoT data to validate the OpenSim results. Two military relevant loaded conditions and magnitudes were selected for their known impact form literature on gait mCoT and kinematics [4] [8]. A no-load condition was added as reference, resulting in three simulated and tested conditions: Unloaded, representing PT outfit, a condition with 1 kg added to each foot (Foot load) as a simulation of increased weight of combat boots, and a condition where 30 kg is added to the trunk (Trunk load). In the latter load condition, the load is distributed between body armor (12 kg) and a compact mass (18 kg) located low in the backpack. In the simulation models, the equipment pieces are modeled as point masses, located at the expected COM of the equipment piece, and rigidly attached to the MSK model.

TABLE I: Load location names with magnitude, location(x = sagittal axis frontal+, y = vertical axis upward+, z = frontal axis right+), Body segment w.r.t. which the load is rigidly attached (Head-Arms-Trunk [HAT COM] or Foot COM).

Load name	Location [x,y,z] (m)	w.r.t. body:	Magnitude (kg)
Backpack (Used in Trunk load)	[-0.19, -0.26, 0]	HAT COM	18
Body armor (Used in Trunk load)	[0,-0.14,0]	HAT COM	12
Boot (Used in Foot load)	[0,0,0]	Foot COM	1 (per foot)

Experiment design

6 young adult, non-military, healthy subjects volunteered and gave written informed consent. The data of 1 subject was excluded for having non-continuous GRF data due to a bad cable connection. This resulted in the following group: 1
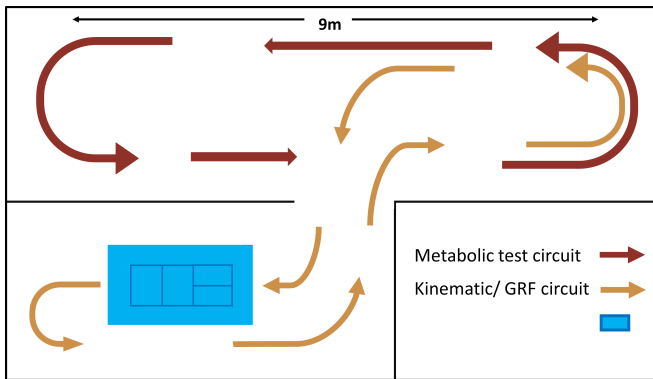
Fig. 1: Test circuit layout

(a) Trunk load condition with the marked location of COM.

(b) Trunk load condition with the marked location of COM.

(c) Foot load condition

Fig. 2: Method of application of load conditions

female/ 4 male, mass = 81.8 ± 14.0 kg, height = 184 ± 7.6 cm. Each subject tested in all the load conditions. All subjects were allowed as much time as necessary to familiarise themselves with walking in the loaded conditions while wearing the necessary sensors. The experiment started directly after the familiarisation process concluded.

The test consisted of two parts. In the first part, each subject was instructed to walk at 1.5 m/s around a circuit of ~20m for 6 minutes to reach metabolic steady state [8]. Only metabolic data was measured during this part of the test. The second part consisted of walking around the same circuit, expanded with an extra loop across an array of force plates (see Fig. 1), so kinematic and GRF data could be collected. Velocity was kept constant throughout both parts of the test by a researcher who verbally instructed the subject to speed up or slow down. The instructions were based on whether the subject reached regularly spaced intervals at beeps of a metronome heard only by the researcher. The metronome could not be heard by the test subject to avoid stepping to the rhythm of the metronome, thereby influencing stride frequency and length. After both parts of the test concluded, the load condition was removed and the subjects were asked to sit and rest for 10 minutes before the next test, to avoid any fatigue effects [8]. Then, the next load condition was tested.

Applying the Foot load was done by taping lead strips around around each shoe (1 kg), see Fig 2c. Trunk load condition consisted of a ballistic vest with soft and hard ballistic plates (10 kg total), additional pouches on the front of the vest simulating ammunition and other utilities (2 kg), and a backpack with a box of exercise weights (18 kg), see Figs. 2a, 2b. The study was approved by the Delft University of Technology Human Research Ethics Committee.

During the experiments, between 17-34 straight steps were recorded for each participant in each load conditions. The exception being one subject's Foot load condition, where the pelvic IMU shifted early on in the recording, so the Xsens suit was no longer correctly calibrated. This data was excluded. All analysed steps were within $0.05m/s$ of the target $1.5m/s$.
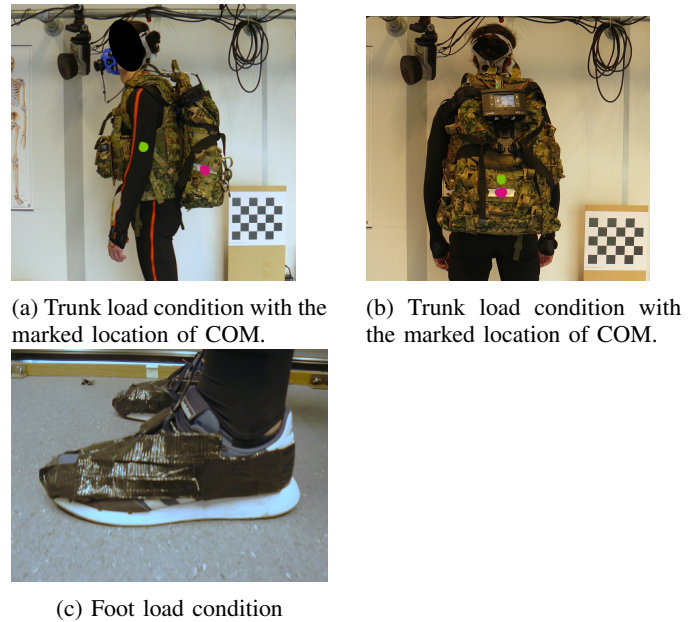
Kinematic measurements: Gait kinematics were measured with a motion tracking suit, which uses 17 IMU based tracking sensors for the body segments (Xsens, MVN Link [16]). This system was proven to be accurate for over ground walking [17] and it was therefore used for the kinematic measurements, instead of optical marker tracking, to avoid optical marker tracking issues caused by the applied load conditions [15]. IMU data is collected at 240 Hz. The sensors are placed on a full body suit in dedicated pockets on each body segment (feet, shanks, thighs, pelvis, sternum, head, shoulder, upper arms, forearms, hands). Straps are placed over the IMU's in the suit to further minimise any cloth movement in the motion tracking data.

GRF measurement: GRF data is recorded at 500Hz by four triaxial force plates using piezoelectric force gauges (KISTLER). These force plates are embedded in a walkway and measure a total surface area of ~1500mm x 600mm (See Fig. 1) Two subsequent foot contacts are be registered in this setup, meaning continuous GRF data from heel-strike (HS) to contra-lateral toe-off (TO).

All combinations of load condition and subject had at least one stride of complete and continuous kinematic and GRF data, except for the Foot load of the subject with the shifted IMU, who's data was not used in metabolic calculations.

Metabolic measurement: To measure the metabolic rate, indirect calorimetry with a COSMED K5 portable gas analysis system is used (COSMED, Rome). The system is recalibrated for each subject, according to instructions of the manufacturer. The COSMED K5 measures oxygen uptake (VO_2 in $ml/kg/min$) and CO2 exhaled (VCO_2 in $ml/kg/min$) and both were measured breath by breath (BxB) over the 6 minutes walking trial.

During the experiments, metabolic steady state was reached by all participants in all load conditions, see Appendix A. *Anthropometric measurement:* The segment lengths of each subject are required by Xsens to correctly scale the model. The measurements are done based on bony landmarks, as instructed by the manufacturer of the Xsens suit.

Gait kinematics and GRF prediction

The modelling of loaded gait kinematics and GRFs is performed by SCONE [12], using the hyfydy plugin [11] for optimisation. In its forward dynamics simulations, this software uses the covariance matrix adaptation evolution strategy (CMA-ES) [18] to optimise the initial states of the musculoskeletal model and the parameters of the muscle controller.

Musculoskeletal model and controller: A 7 segment musculoskeletal (MSK) model is used, with 9 degrees of freedom (DOF) and 9 muscle-tendon units (MTU) per leg: mm. Hamstrings (grouped into one MTU), m. Biceps femoris (short head), m. Gluteus maximus, m. Iliopsoas, m. Rectus femoris, mm. Vasti (lateral and medial grouped in one MTU), m. Soleus, m. Gastrocnemius and m. Tibialis anterior. Viscoelastic Hunt-Crossley contact spheres [19] are modeled at the calcaneus and metatarsophalangeal joints of the foot for GRF calculations, see Fig. 3. This model is planar in the sagittal plane, which highly reduces the number of DOF and muscles needed to be optimised and thus the computational time and effort required. Most noticeable changes for loaded kinematics are expected to be in this plane [3] [4] [8], so the impact that the low number of DOF and muscles has on simulation results should be minimal. This MSK model can be found as the H0918v3 model in the SCONE repository. The model is scaled to the mean anthropometry and mass of the 5 subjects of the experiment. The 18 muscles in the model are controlled by a reflex-based muscle controller as proposed by Geyer and Herr [20]. This controller optimises initial states and force- /length based reflexes of each muscle in two gait states: swing and stance phase. In earlier studies, it has been shown to be achieve robust muscle control and reproduce the salient features of human gait in different speeds, environments [21] and also for loaded gait [9].

CMA-ES and the objective cost function: The CMA-ES used by SCONE applies a multi-objective cost function (OCF) to evaluate each simulation, based on how well the simulation meets a set of objectives (J). All combinations of initial states and parameter values have their own J score and the solution space for all combinations is therefore large. The way CMA-ES in SCONE solves this optimisation problem, is roughly described by the following sequence:

1) 'Guess' a random combination of parameter values (m_0).
2) Create a population (λ=10) of points with different parameter set values distributed around m_0.
3) The spread and direction of how these points are distributed around m_0 is the Covariance matrix.
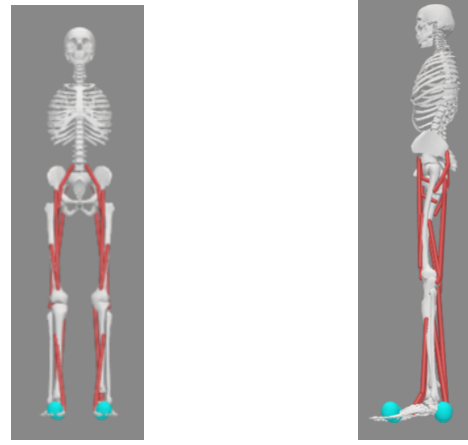

Fig. 3: Musculoskeletal model used for kinematic modelling

4) Evaluate the points in λ and find which have the best J score.
5) 'Guess' a new m based on the best performing points (μ) and their parameter sets. The covariance matrix of points around this new m_1 is based on how μ relates to λ.
6) Continue with 2-5 and repeat until the mean progress of J score of m_n to $m_{(n+500)}$ reaches a certain minimum threshold.

Each optimisation converges to a single optimal point, which may be the global optimum or a local optimum. Multiple parallel optimisations can be done in SCONE, which can increases the number of optima found and the likelihood that the global optimum is one of the found solutions.

The OCF in this study contained 7 objectives. These objectives either try to ensure realistic kinematics and GRFs, or try to minimise the required muscle effort and fatigue, two factors that are noted as reasons for optimisation of gait [22]. The OCF used for this study is:

$$J = w_v * J_v + w_{knee} * J_{knee} + w_{ankle} * J_{ankle} + w_{head} * J_{head} + ...w_{GRF} * J_{GRF} + w_{eff} * J_{eff} + w_{act} * J_{act}$$

With:

$$J_v = \frac{1.5 - V_{avg}}{1.5}$$

Objective to achieve walking velocity of 1.5 m/s. No movement scores 1, while gait at 1.5 m/s scored 0. A threshold was set at $J = 0.02$, meaning all velocities between 1.47-1.53 m/s were considered acceptable.

$$J_{knee} = T_{knee} \text{ (when } \theta_{knee} = 0 \text{ deg)}$$

When the knee angle becomes 0, any torques that might force hyperextension are penalised.

$$J_{ankle} = \left\{ \begin{array}{ll} |\theta_{ankle}| - 60, & \text{if } |\theta_{ankle}| > 60 \\ 0, & \text{if } |\theta_{ankle}| \leq 60 \end{array} \right\}$$

Any ankle angles larger than 60 deg plantar- or dorsiflexion are penalised.

$$J_{head} = |\dot{\theta}_{pelv.tilt}|$$

The term was added to emulate the tendency of humans to stabilise their head during gait [23] Head movement was detected by the angular velocity of the pelvis tilt, as the trunk and head formed a single segment. Threshold was set at a score of 0.5 so any angular velocities larger than 0.5 rad/s were penalised.

$$J_{GRF} = \left\{ \begin{array}{ll} F_{y_{max}} - 1.2, & \text{if } F_{y_{max}} > 1.2 \\ 0, & \text{if } F_{y_{max}} \leq 1.2 \end{array} \right\}$$

This term is added to avoid unrealistic high GRF impact peaks at HS. GRF is normalised for body weight and threshold was set at 0.1 so impact peaks higher than 1.3 were penalised.

$$J_{eff} = \dot{B} + \sum_{n=1}^{18} \dot{EE}_n,$$

This term is the metabolic cost of transport, as defined by Wang *et al* [21] Where $\dot{B}$ is the basal metabolic rate of 1.51 times body mass [24] and $\dot{EE}_n$ is the average metabolic energy expenditure of muscle n, as defined by Bhargava *et al* [25].

$$J_{act} = \int_{t=0}^{t_{end}} [\sum_{n=1}^{18} activation_n(t)^2] dt$$

Quantification of muscle fatigue, as defined by Veerkamp *et al* [22], represented as the sum of all integral muscle activations squared.

Initial weights were taken from an example OCF in the SCONE repository, and tuned empirically with a target to consistently achieve normal gait patterns in the Unloaded condition. The result was the following set of weights:
$w_v = 1000$ $w_{knee} = 0.02$, $w_{ankle} = 0.1$, $w_{GRF} = 10$, $w_{head} = 10$, $w_{eff} = 0.1$, $w_{act} = 2000$
These were kept consistent for all load conditions.

Gait simulation: To achieve the best possible result and increase the chance of finding the global optimum, the following process is used:

1) Initial optimisation
   - For each load condition, the base muscle controller as proposed by Geyer and Herr [20] is optimised using a simplified OCF:
     $J = J_v * w_v + J_{knee} * w_{knee} + J_{ankle} * w_{ankle} + J_{eff} * w_{eff} + J_{act} * w_{act}.$
   - When a model achieves stable gait at 1.5 m/s, the simulation is terminated.

2) Intermediate Optimisation
   - The $w_{GRF} * J_{GRF}$ term is added to the OCF.
   - The optimised states and controller parameters of the initial optimisation are set as the initial parameters of the m_0 of a new optimisation. The standard deviations of the Covariance matrix are reset. This allows the new optimisation to find more optimal parameters that achieve gait at 1.5 m/s, thus reducing the chance of all parallel optimisations converging to one minimum.
   - Three parallel optimisations are performed until the normalised peak GRF of the stable gait remains lower than 1.3.

3) Final optimisation and selection
   - $w_{head*}J_{head}$ term is added to the OCF.
   - The solutions from the three intermediate parallel optimisations are set as the m_0 for three new optimisations, covariance matrix standard deviations are reset.
   - Five parallel optimisations are performed for each of the three initial parameter sets, using the full OCF, until the progress of improvement of the OCF score reaches a threshold of 10^{-5}. In total, 15 optimisation results are obtained using the full OCF for each load condition
   - Of all total simulations for each load condition the four results with the lowest OCF score are used to compare to the measured data.

This strategy has a number of benefits over setting the amount of parallel optimisations of the initial optimisation to 15. First, the total simulation time is lower, as the λ point sets of all 15 final optimisations are already in the direction of the solution space which achieves stable 1.5m/s gait with reduced GRF peaks. This strongly reduces the time spend on optimisations which would never reach those objectives. Secondly, by focusing the 15 λ sets in directions of the solution space which do achieve these objectives, the solution space in that direction is evaluated more thoroughly, improving the chance of finding the global optimum. The strategy of applying intermediate optimisations is not known to have been used before in loaded gait simulations.

Metabolic cost of transport estimation

The metabolic cost of transport quantifies the energy expended during movement, which can be estimated using the OpenSim modelling software [10]. From input gait kinematics and corresponding GRFs, the Computed Muscle Control (CMC) algorithm can calculate the muscle activations and forces required for an MSK model to track the input motion. From the CMC results, the mCoT can be calculated.

Musculoskeletal model: For the kinematic and GRF modelling, the MSK model is kept as simple as possible to reduce simulation time, hence a planar model with only 18 muscles is used there. Because a reduction of simulation time is less of a priority for the mCoT modelling, as less simulations will be performed, a non-planar and more complex MSK model is chosen, allowing for 3D tracking of the input kinematics. A 3D model has more DOF and thus necessitates more muscles to control all DOFs. The chosen MSK model uses 40 muscles per side and controls 39 DOF [26], see Fig. 4. It applies Hill-type muscle models as specified by Millard *et al* [27], which incorporate maximum isometric force, optimal fibre length, tendon slack length and
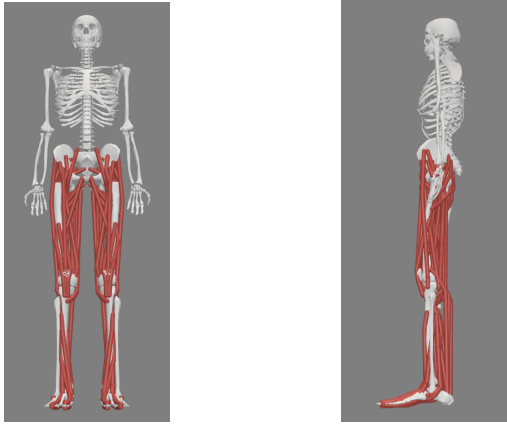
5

Fig. 4: Musculoskeletal model used for metabolic modelling

pennation angle muscle parameters, and accounts for activation dynamics and contraction dynamics. All muscle parameters of the MSK model used in this study are as stated by Rajagopal *et al* [26].

Metabolic calculation: The dimensions of the MSK model are scaled to match the anthropometry of the test subject who's measured data is used for each simulation. Reserve actuators are added to each DOF to ensure sufficient control to track the input kinematics and GRFs. The control effort required by these actuators is subsequently reduced by OpenSims Reduce Residual Algorithm (RRA). RRA takes input kinematics and GRFs, calculates and then reduces the required torques to track the input data. It does this by adjusting the COM locations of the torso and by slightly altering kinematics. For this study the RRA process is repeated until mean residual forces on the pelvis are below 10N. The adjusted MSK model and kinematics are then input in the CMC algorithm of OpenSim. CMC uses feedback control to estimate future accelerations of joints required to track the desired motion. It then calculates the optimal muscle force and activation to achieve these accelerations using static optimisation, while muscle activation dynamics are taken into account [28]. CMC is calculated from TO to HS of the contra-lateral side, to avoid high residual actuator forces required to compensate for the missing GRF data in the double leg support phases before first TO and after second HS. Note that this is less than one full stride, as one single-support-phase is not measured. Converting the muscle activity to metabolic energy is done for each muscle, based on the 2010 revisions [29] of the muscle energy expenditure model by Umberger *et al* from 2003 [30]. This model takes the muscle parameters from the MSK model, contraction velocities and exerted forces from the CMC calculations, and estimates the total expended energy ($\dot{EE}$), by the following formula:

$$\dot{EE} = \dot{w}_{CE} + \dot{h}_A + \dot{h}_M + \dot{h}_{SL}, [W]$$

thus accounting for: Mechanical work done by the contractile element ($\dot{w}_{CE}$), activation heat rate ($\dot{h}_A$),

shortening/lengthening heat rate ($\dot{h}_{SL}$), maintenance heat rate ($\dot{h}_M$) and a basal heat that accounts for non-movement related physiological processes. Two main alterations to the metabolic muscle model are implemented, as proposed by Uchida *et al* [31], namely to include negative mechanical work and to implement a similar muscle recruitment strategy as by Barghava *et al* [25]. This metabolic muscle model has been validated for various different motions, including walking with assistive devices [32] and various hopping tasks [33].

Data processing

Experimental kinematic data: The joint angles and virtual kinematic marker data from the Xsens suit are exported. Virtual markers are placed by Xsens according to the measured anthropometry of the subjects. Scaling of the MSK models in OpenSim during the mCoT estimation process can therefore be performed based on these markers.
For the SCONE result validation, the joint angle data used (pelvis tilt and hip, knee and ankle angle) filtered at 6 Hz using a 4th order low-pass Butterworth filter and then separated into stride data, from HS to ipsilateral HS. Only experimental motion data from straight steps around the circuit is used. HS detection is done by a foot velocity algorithm (FVA). HS is detected when the absolute vertical and forward velocities of Xsens' virtual heel center marker drop below 0.1 m/s. This algorithm is similar to the one used by O'Connor *et al* in their 2007 study [34], which is considered to be highly accurate for normal gait (RMS < 20ms). All stride times are then normalised to the gait cycle and combined into one dataset for each load condition.

Experimental calorimetry data: COSMED data is low-pass filtered using a moving average filter with a window of 15 breaths ($\sim$ 5s), as is often used in BxB data analysis to remove outliers [35]. Data of the last minute is then averaged to obtain steady state values of VO2 and VCO2 in ml/min, in each load condition. The steady state average is subsequently divided by the walking velocity and normalised for body weight. Brockway's equation [36] was used to convert the O2 and CO2 data to mCoT:

$$mCoT = 16.51 * VO_2 + 4.51 * VCO_2, [J/kg/m]$$

Kinematics and GRF modelling results: Joint angle data and GRF data of the four best performing SCONE/hyfydy optimisation runs of each condition are exported from SCONE, and separated into stride data from HS to ipsilateral HS. The calcaneus velocities as defined by SCONE are used in this case to detect HS with the same FVA as used for processing of the experimental kinematic data. The duration of each stride is then normalised to the gait cycle and combined in a dataset for each of the four best optimisations.
Metabolic cost of transport modelling input and result: Virtual marker data from Xsens is tracked using Inverse Kinematics in OpenSim. The resultant kinematics and the
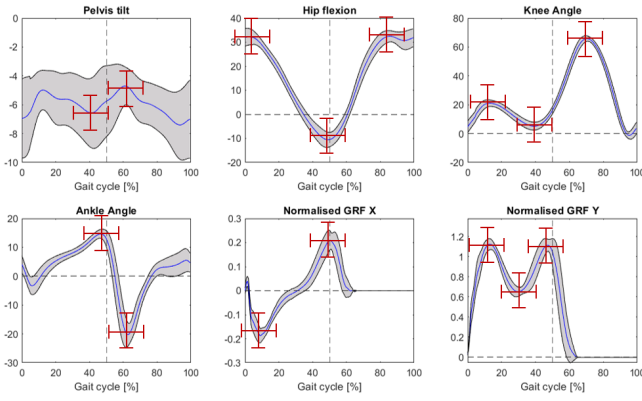
Fig. 5: Peaks analysed for trends between load conditions: Horizontal and vertical bars indicate respectively time and value is analysed for that peak.

GRF data required as input for the CMC are initially not synchronised, as they originate from different measurement and coordinate systems (Xsens and Qualisys/Kistler). To align both datasets, centre of pressure (COP) coordinates from the Kistler force plates are low-pass filtered using a 4th order butterworth with a cutoff frequency at 6Hz, resampled and then matched to the Xsens kinematics using the following process:

- HS coordinates of a stride are registered for both systems and a vector is defined between both HS in their own coordinate system.
- Both vectors are translated so the HS of the right foot is at the origin of its own coordinate system.
- The angle between both vectors is calculated and the GRF data is rotated accordingly to match the kinematic data.
- Timestamp of the GRF data HS is matched to the timestamp of kinematics HS.

When a foot is placed on two force plates, then the data of both is combined. Forces of both plates are summed and centre of pressure (COP) data is averaged between the two plates.

From the $\dot{EE}$ estimations by OpenSim, mCoT is calculated according to the following formula:

$$mCot = [\sum_{n=1}^{80} \int_{t_1}^{t_2} \dot{EE_n}]/(M_{body} * v), [J/kg/m]$$

Where EE_m is the energy expended by muscle n, M_{body} is the body weight of the MSK model without applied load and v is the gait velocity. t_1 and t_2 are mid-stance (MS) 1 and 2. As no full stride data is available, the mCoT data of one step is used, this still entails a full stance and a full swing phase, and is thus representative for mCoT in gait, assuming symmetrical gait.

Analysis & Validation

Instead of comparing absolute values of kinematics, GRFs and mCoT between experimental and simulated data, the trends from load condition to load condition within simulated results are compared to those observed between measured results. 'Trend' throughout this study is defined as the characterisation of differences from load condition to load condition, specifically, an analysed parameter that shows a significant difference between load conditions. 'Trend direction' is whether the difference is an increase or decrease of the parameter value.

Kinematics and GRF prediction assessment: Of each joint angle in the sagittal plane (Pelvis tilt, hip, knee and ankle flexion), and of vertical GRF and forward GRF, 2-3 peak values and their moment of occurrence in the gait cycle are analysed. In total, stride length and 30 angle and force peaks are analysed. Which peaks of each measure are analysed exactly is shown in Fig. 5.

Statistical analysis: The peaks of all steps in each load condition dataset are compared to those of the other load conditions, using a repeated measures ANOVA, where appropriate. Any significant differences ($p \leq 0.05$) will be subsequently analysed using a post-hoc Bonferroni correction.

For the simulated kinematics and GRF data, all the steps from the four best simulated runs will be combined into one dataset for each load condition. Statistical analysis for trends between load conditions is then the same as for those between the experimental data.

The threshold values to be regarded as a difference are as follows: $3°$ for joint angles [37], 1% of the mean normalised GRF ($\sim$ 8N/0.8 kg) and 2% of gait cycle for timing differences, as per the Nyquist criterion since SCONE samples at 100 HZ (50Hz $\sim$ 2%).

Validation: Analysing a parameter for trends can have can have five possible outcomes: correctly predicted trend and direction, correctly predicted no trend, correctly predicted trend but opposite direction, incorrectly predicted trend, incorrectly predicted no trend. The model is considered an accurate model when the following two criteria are met:

1) Correct predicted, trend and no trend > 80% of total.
2) No predicted trends in opposite direction.

Metabolic cost of transport estimation assessment: Measured and estimated mCoT are both analysed for trends between load conditions.

Statistical analysis: The two loaded conditions are tested for significant ($p < 0.05$) differences from Unloaded using the Kruskal-Wallis test, with Dunn's post-hoc test.

Validation: An earlier study by Dembia *et al* [32] from 2016 modelled assistive devices to carry a trunk load in OpenSim, using the same MSK model and mCoT calculations. They found that these calculations typically underestimated mCoT by 11% and underestimated changes from no-load to a loaded condition by 8%. This tendency for underestimation

was later confirmed by a study comparing different metabolic models [38].

The current method is expected to be less accurate then the estimations by Dembia *et al*, due to the need for synchronisation of kinematics and GRF. Any errors in that process are expected to increase the estimated mCoT. The predictions of this method are therefore considered accurate when the following criteria are met:

1) All mCoT trends and trend directions between load condition found in experimental data are also found in the simulated mCoT

2) The model underestimates the difference of estimated mCoT between unloaded and Foot/Trunk conditions by 0-8%.

RESULTS

Gait kinematics and GRF prediction

All 15 final optimisations reached stable gait at $1.5m/s$, ($\pm0.03m/s$). All optimisations took between 1500 - 2500 generations to reach the threshold progress and the average optimisation time was 23 minutes until threshold progress was reached. The four best scoring optimisations originated from different intermediate optimisations in all load conditions.

Experimental and simulated kinematics and GRFs are presented in Fig. 6.

56/93 ($\sim60\%$) of expected trends between load conditions from experimental data were also correctly predicted by the simulated results. False negatives and false positives together made up 33/93 parameters, while 4/93 predicted the opposite of the expected trend direction. The full comparison between the measured trends and the trends form the combined simulation runs is shown in Fig. 7.

A visual representation of the trend directions of each parameter is presented in Appendix B.

Metabolic cost of transport estimation

After synchronisation of both datasets, visual inspection showed that not all GRF vectors were correctly matched to the foot and some manual adjustments were required for 10/14 processed steps. After the adjustments, RRA and CMC ran successfully for all combinations.

From experimental data, significant differences between both loaded conditions and Unloaded are expected while no significant differences were found in the estimated mCoT by the metabolic cost of transport estimations. Full comparison of results between the measured mCoT and the estimated mCoT from OpenSim in the three load conditions are presented in Fig 8.

DISCUSSION

Gait kinematics and GRF prediction

The first aim of this study was to predict biomechanics of loaded gait, and check whether simulated results correlate with experimental data. Only $\sim60\%$ of the measured trends were correctly predicted by the simulation and 4 of the incorrect predictions were in opposite direction of measured expectation. Therefore, the applied modelling method as a whole cannot be considered accurate.

When looking past the amount of incorrect predictions, there are some encouraging results found in this simulation strategy. From Fig. 7 it can be observed that for the Foot load condition compared to Unloaded, the expected outcomes from literature of increased stride length [8] and increased knee flexion [39] were correctly predicted by the model. Similarly for the Trunk load condition, the expected results of increased forward trunk lean and range of motion (difference between max and min angle of the pelvis) [40] and of decreased stride length [7], were all correctly predicted as well. When looking at the number of measured trends in each of the three comparisons between conditions, Unloaded - Foot has the least (4/31) while Foot - Trunk has the most (21/31). The simulation results also show this pattern.

The majority (25/37) of incorrectly predicted trends are false positives, which indicates that the model tends to overestimate kinematic and GRF differences between load conditions. An explanation for the incorrect predictions could be the simplified 2-state gait-state controller used in the simulations. This controller only has a 'swing-phase' state and a 'stance-phase' state, determining the optimised muscle and DOF reflexes. This results in a stance-phase where, for example, the leg always tends to extend, while the extension reflex of the stance leg in 'early-stance' phase is not quite as aggressive, which creates differences in joint angles between the predicted and measured kinematics. When looking at knee angle trajectories in Fig 6, it can be observed that this effect is the same in Unloaded and Foot load condition, but is not present during Trunk loading. The heavy load requires more effort to extend the knee, which results in an angle pattern more similar to experiment data for that condition. Similarly, a lack of distinction between 'early' and 'late swing' directly influences parameters trends in hip and knee angles in the second half of the gait cycle. These errors do not remain localised, due to error propagation throughout the kinematic chain, possibly affecting more parameters. For example, the later timing of the 'Knee flexion max 1' in Trunk load compared to Unloaded, could be the cause for the unexpected later timing 'Hip flexion max 1' and 'Forward GRF min'.

The variance in kinematics/GRFs (Fig 6) of the four best performing optimisations indicate that there are different solutions that result in similar OCF scores. This highlights the value of the applied optimisation strategy for analysis of loaded gait compared to unloaded, using intermediate optimisations and combining a subset of the best. Comparing only a single optimisation from each condition, as done by Dorn *et al*, could provide rather different trend results dependant on the optimisation, thus influencing the analysis of the impact of load conditions on kinematics and GRFs.
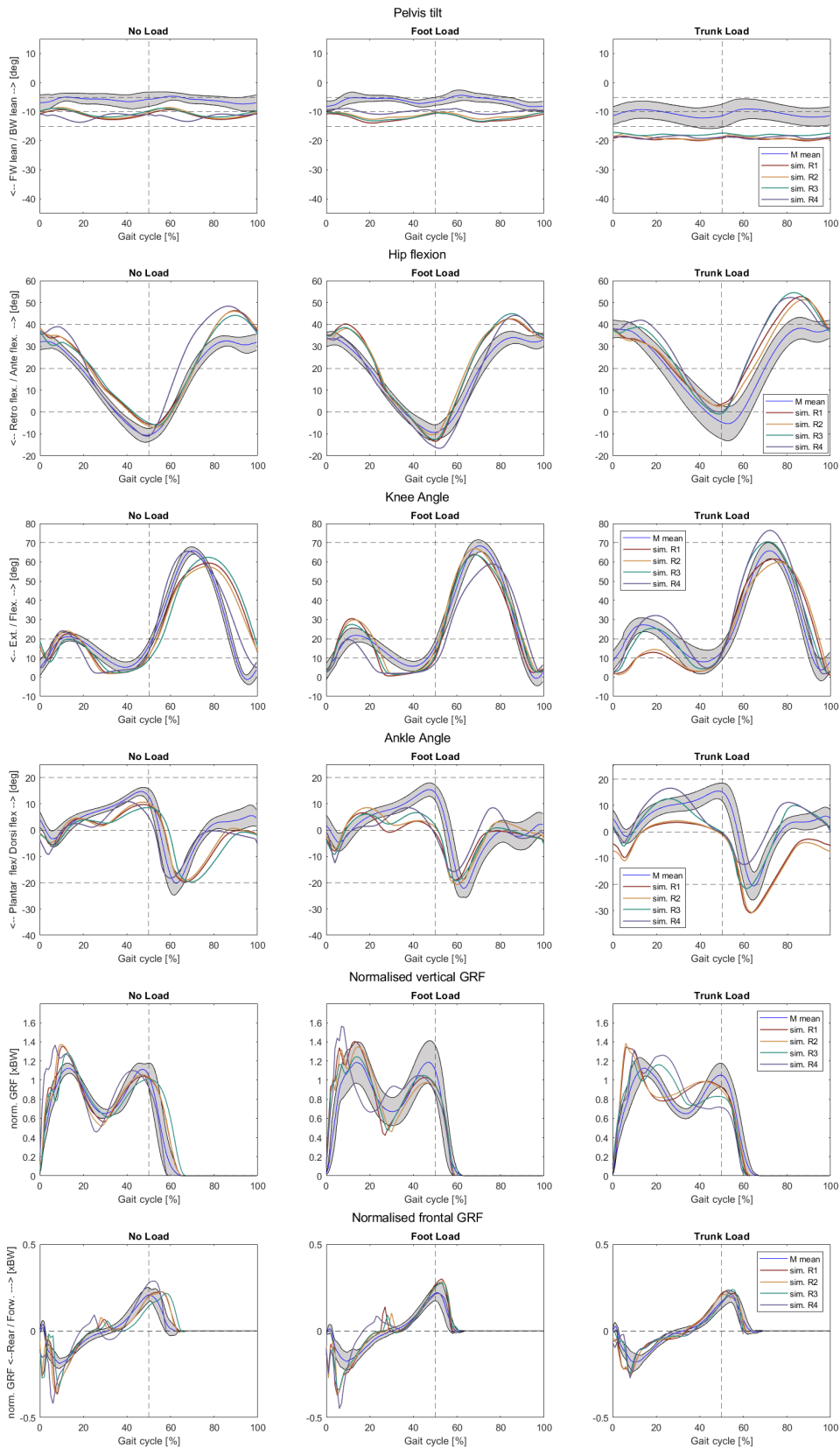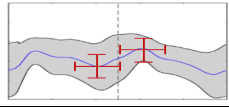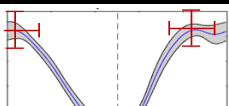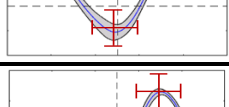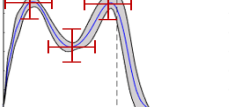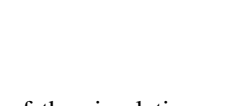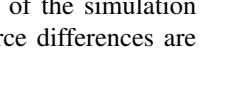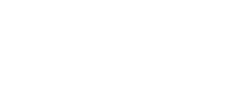
Fig. 6: Comparing measured and simulated kinematics and GRF. 'M mean' in the legend is the experimental mean joint angle. Gray shaded is the SD of experimental data. Coloured lines are averages of the four best performing simulation runs (sim. R1 - R4)

Parameter	Unloaded --> Foot Measured +/-	diff	Simulated +/-	diff	Unloaded --> Trunk Measured +/-	diff	Simulated +/-	diff	Foot --> Trunk Measured +/-	diff	Simulated +/-	diff
Trunk angle max	=	=	=	=	-	-3,974	-	-8,374	-	-4,052	-	-7,666
Trunk angle max (t)	=	=	=	=	=	=	=	=	=	=	=	=
Trunk angle min	=	=	=	=	-	-3,931	-	-6,504	-	-3,071	-	-6,417
Trunk angle min (t)	=	=	=	=	=	=	=	=	=	=	=	=
Hip flex max 1	+	2,331	=	=	+	6,822	=	=	+	5,490	=	=
Hip flex max 1 (t)	=	=	+	8,538	=	=	+	6,336	=	=	=	=
Hip flex min	=	=	-	-4,863	+	6,862	+	9,238	+	5,778	+	15,078
Hip flex min (t)	=	=	=	=	+	4,017	=	=	+	3,290	=	=
Hip flex max 2	=	=	=	=	+	6,652	+	7,192	+	5,212	+	9,979
Hip flex max 2 (t)	=	=	=	=	=	=	=	=	+	4,187	+	4,733
Knee flex max 1	=	=	+	6,608	+	6,982	=	=	+	6,112	-	-3,196
Knee flex max 1 (t)	+	3,329	+	4,174	=	=	+	10,981	=	=	+	8,413
Knee flex min	=	=	=	=	+	3,673	=	=	+	3,213	+	3,241
Knee flex min (t)	=	=	=	=	+	3,208	+	9,141	+	2,836	+	11,207
Knee flex max 2	+	3,470	+	4,666	=	=	+	8,277	=	=	+	6,061
Knee flex max 2 (t)	=	=	=	-3,561	=	=	=	=	=	=	+	4,733
Ankle angle max	=	=	=	=	=	=	=	=	=	=	=	=
Ankle angle max (t)	=	=	-	-15,761	=	=	-	-16,186	=	=	=	=
Ankle angle min	=	=	=	=	=	=	=	=	=	=	=	=
Ankle angle min (t)	=	=	-	-5,466	+	2,188	-	-3,052	+	2,099	+	3,543
Forward GRF min	=	=	=	=	=	=	+	0,121	=	=	+	0,142
Forward GRF min (t)	=	=	=	=	=	=	+	2,639	=	=	+	2,955
Forward GRF max	=	=	=	=	=	=	=	=	=	=	=	
Forward GRF max (t)	=	=	=	=	+	4,508	=	=	+	4,696	=	=
Vertical GRF max 1	=	=	+	0,097	=	=	=	=	=	=	-	-0,031
Vertical GRF max 1 (t)	=	=	+	3,073	=	=	=	=	=	=	-	-2,508
Vertical GRF min	=	=	=	=	=	=	+	0,249	=	=	+	0,294
Vertical GRF min (t)	=	=	=	=	+	4,526	+	5,133	+	5,142	+	7,635
Vertical GRF max 2	=	=	=	=	=	=	-	-0,049	-	-0,015	-	-0,019
VerticalGRF max 2 (t)	=	=	=	=	+	3,592	-	-8,689	+	4,298	-	-6,202
Stride length	+	0,045	+	0,185	-	-0,070		-0,285	-	-0,115	-	-0,100
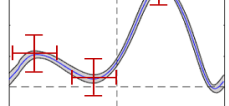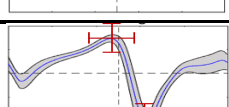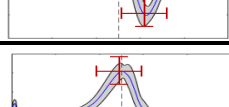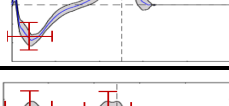
Correct difference & direction	21	Opposite to meas. trend	4
Correct no difference	35	Incorrect a difference	25
		Incorrect no difference	8

Fig. 7: Comparison between kinematic and GRF measured trends and the trends of the combined average of the simulation runs. Angle differences are in degrees, time (t) differences are in % of gait cycle, length in meters and force differences are normalised to body weight. Note: negative trunk angle corresponds to forward lean.
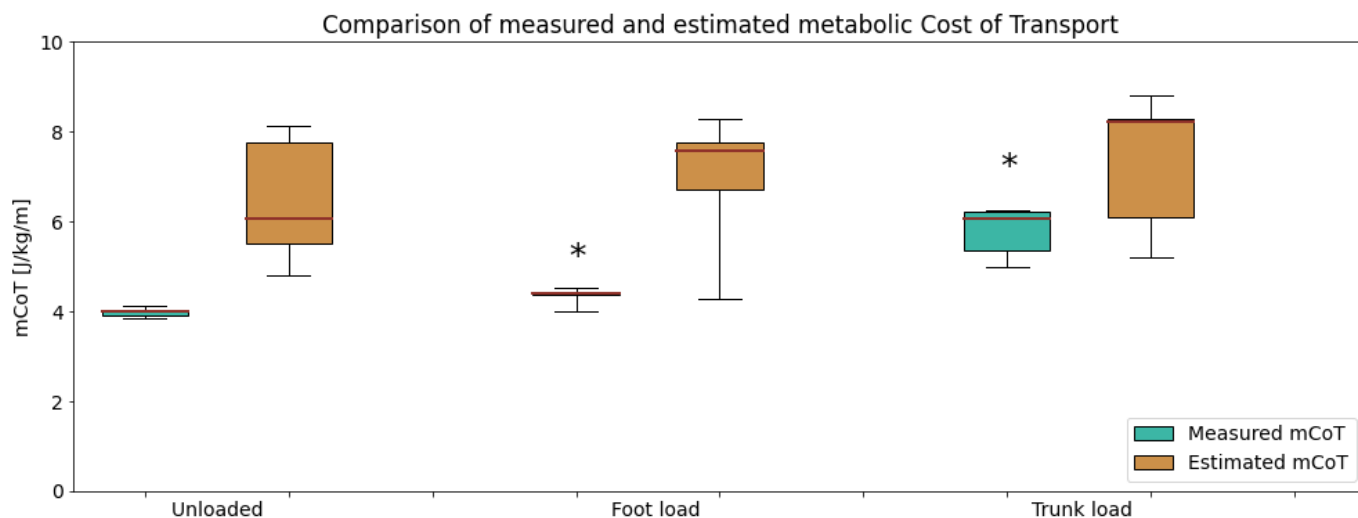
Fig. 8: Experimental mCoT data and OpenSim estimated mCoT compared. Whiskers show min and max values. (*) Indicates a significant ($p < 0.05$) difference from the unloaded condition.

The impact of diverging kinematic/GRF solutions diminishes when the four best simulations are combined, thus making the result more robust, although combining more optimisations than four is likely to increase this effect even further. Increasing the optimisations is already possible looking at simulation times achieved in this study. Increasing the parallel optimisations of the intermediate OCF from 3 to 5 and optimising each 6 times rather than 5 would require roughly as much simulation time for 30 full optimisations as Dorn *et al* required for a single optimisation.

Running more simulations will likely reduce the resulting number of false positives/negatives in predicted trends, as the variability of the best performing optimisations is expected to be lower, and on average closer to the global optimum. Increasing the number of gait states in the controller would improve the results further, as some structural errors in the model are removed. Note however, that this could come at the cost of a longer simulation time, as the more complex controller possibly takes longer to achieve stable gait. Further research is required to assess the actual impact on results of both improvements to the methodology.

Recommendations:

Increased number of gait states: Solving the issues caused by the low number of gait states could be achieved by expanding the used controller to five states: 'Early-stance', 'mid-stance', 'late-stance', 'early-swing' and 'late-swing'. More states than five are expected to yield limited further improvements due to the stride time of ∼1s and the 6Hz upper limit of human motor control adaptability.

Increase number of simulations: Running more intermediate and total OCF optimisations would improve the results by providing more data points and reduce the impact of less-optimal local minima. For doubling of the included simulation runs, the following sequence of parallel optimisations is recommended:

1) 1 optimisation of the model to the base OCF.
2) 5 optimisations of 1)'s results, to OCF + J_{grf}
3) 6 optimisations of 2)'s results, to OCF + $J_{grf} + J_{head}$
4) Combining 6-8 best performing optimisations.

Metabolic cost of transport estimation

The second aim of this study was to estimate mCoT in each load condition, based on experimental IMU based kinematics and force plate GRF input data, and assess whether those results line up with measured trends. None of the significant differences from experimental data were found in the estimations of mCoT.

The origin of these observed discrepancies must lie in the kinematic and GRF data input in OpenSim, as the experimental mCoT through indirect calorimetry match quite well with literature [5] [8], and the OpenSim RRA/CMC method of mCoT estimation has produced more reliable results in earlier studies [31] [32], which more closely matched experimental results. Specifically, these discrepancies are probably the result of many errors along the data measurement and processing chain. Relevant errors include the following: Motion tracking errors, for example those caused by soft tissue movement [41] or magnetic disturbances [42], inaccuracies in GRF COP and force data when a foot was placed on two force plates at once and finally, rounding errors caused by filtering, resampling datasets and transformations during dataset synchronisation. These errors compound which results in low spatial correlation between kinematic and GRF data, subsequently preventing OpenSim from producing accurate results. Although these errors are often not expected to be large, CMC is a process sensitive to errors. A small difference in location or direction of the GRF vector can often mean opposing joint moments to those required for normal gait, as a 3° error in both hip and knee could very well result in a

4-6cm discrepancy between kinematic and GRF data. Compensating for the wrong location of the GRF vector requires highly atypical muscle activation, resulting in a much higher mCoT. Upon inspection, muscle activation patterns and levels of the Unloaded simulations, were indeed highly atypical for healthy gait, See Appendix C-1. m. Semimebranosus, m. Semitendinosus, mm. Vasti, m. Biceps femoris, m. Rectus femoris and m. Soleus, at some point were all active at unexpected points in the gait cycle of a simulation, when compared to experimental EMG data [43] and other CMC based mCoT estimations [26] [31]. Especially high activity early in stance-phase by m. Semimebranosus, m. Semitendinosus and m.Bicep femoris (long head), affected the mCoT in almost all simulations. A reason for these activations could be a large flexion moment in the hip and lack of flexion moment in the knee, caused by the GRF vector erroneously being located too far forward in this phase of gait. These shifted forces have to be compensated by atypical activation to correctly track the input kinematics, which would explain the activation patterns and levels of the three hip extensor muscles. Comparing GRF data from this study to GRF data in the OpenSim repository of the 2016 Rajagopal *et al* study [26], confirms that the GRF vector indeed was badly matched to the kinematics, See Appendix C-2 for an example.

The inconsistent nature of these errors makes the results of the CMC calculations not only inaccurate but also unreliable, reflected in the large variance of simulated data compared to measured data (Fig 8).

Reducing these errors in future work might prove difficult. For one, alternatives for IMU motion capture in proven technology are limited, with optical marker tracking remaining unpractical for movement with military body borne loads. Even though relatively new technology, such as markerless motion tracking, have shown some promising results [44], a recent Master's thesis presented RMSEs comparable to those expected in IMU based motion tracking for body borne load carriage kinematics [45]. Second, the synchronisation between the kinematic and GRF data will always be a requirement, unless both datasets originate from the same system, something that is currently not known for systems other than lab-bound, optical marker systems that incorporate integrated force plates.

The best solution might be to avoid the separate validation of mCoT estimations altogether. If kinematic predictions, such as these performed by SCONE, become accurate to within 1-2° of experimental data, then using those kinematics with matching GRF could very well be the most valid way of assessing the model, as the mCoT model itself is shown to be able to produce accurate results for unloaded gait [31].

Recommendations:

Kinematic implementation At the moment, validation of the metabolic model for a variety of body borne loads based on experimental input data does not seem feasible. Rather, when deemed accurate enough, implement simulated kinematics and their corresponding GRFs as input for mCoT modelling.

CONCLUSION

In summary, this study set out to model the impact of different body borne loads on kinematics and metabolic performance during walking at 1.5m/s. Both these models were evaluated separately to prospect their suitability to eventually be combined, allowing for performance predictions without the need for experimental data. This would enable the ability to optimise body borne load configurations for performance of military personnel, without the need for expansive and expensive testing. It would also allow for the evaluation of new equipment in a much earlier stage of product design/development, reducing R&D time and cost.

The kinematic predictions showed promising results, as expected difference trends between load conditions from literature were correctly predicted by the model, even with a planar MSK model and a gait state controller using only 2 states. However, opportunity remains for future studies to improve these results, with the highest improvement expected to come when the number of gait states is increased to 5. Additionally, the value of the new strategy combining multiple results stemming from intermediate optimisations is highlighted by presented results. Further increasing the number of carried out optimisations is expected to improve kinematic predictions even further.

It was deemed not possible to validate the metabolic model for walking with body borne loads, based on the current results, as the inaccuracies in the experimental data and those introduced in the processing and synchronisation of kinematic and GRF data prevented OpenSim from producing reliable results. For future work, rather than first validating the metabolic model for loaded walking, implementing the improved simulated kinematics and GRFs directly might produce the most accurate results.

In conclusion, while this study was not able to produce results that conclusively validate either model, it does show promise for future work, enough to continue the work for an integrated approach in combining kinematic and metabolic models. Implementing the recommended alternations to the kinematic simulation strategy provide the first steps to a solid basis for a tool that predicts the impact on military personnel performance of different body-borne loads. In doing so, it paves the way for effective analysis and optimisation of load and equipment configurations, reducing resources required for testing and enhancing military performance.

REFERENCES

[1] J.J. Knapik, E. Harman, and K. L. Reynolds, "Load carriage using packs: A review of physiological, biomechanical and medical aspects," *Applied Ergonomics*, vol. 27, no. 3, pp. 207–216, Jun. 1996, doi: https://doi.org/10.1016/0003-6870(96)00013-0.

[2] R. V. Vitali et al., "Body-worn IMU array reveals effects of load on performance in an outdoor obstacle course," *PLOS ONE*, vol. 14, no. 3, p. e0214008, Mar. 2019, doi: https://doi.org/10.1371/journal.pone.0214008.

[3] B. Liew, S. Morris, and K. Netto, "The Effect of Backpack Carriage on the Biomechanics of Walking: A Systematic Review and Preliminary Meta-Analysis," *Journal of Applied Biomechanics*, vol. 32, no. 6, pp. 614–629, Dec. 2016, doi: https://doi.org/10.1123/jab.2015-0339.

[4] D. Abe, S. Muraki, and A. Yasukouchi, "Ergonomic effects of load carriage on the upper and lower back on metabolic energy cost of walking," *Applied Ergonomics*, vol. 39, no. 3, pp. 392–398, May 2008, doi: https://doi.org/10.1016/j.apergo.2007.07.001.

[5] M. J. Myers and K. Steudel, "Effect of limb mass and its distribution on the energetic cost of running," *Journal of Experimental Biology*, vol. 116, no. 1, pp. 363–373, May 1985, https://doi.org/10.1242/jeb.116.1.363.

[6] . M. Simpson, B. J. Munro, and J. R. Steele, "Does load position affect gait and subjective responses of females during load carriage?," *Applied Ergonomics*, vol. 43, no. 3, pp. 479–485, May 2012, doi: https://doi.org/10.1016/j.apergo.2011.07.005.

[7] J. S. Coombes and C. Kingswell, "Biomechanical and physiological comparison of conventional webbing and the M83 assault vest," *Applied Ergonomics*, vol. 36, no. 1, pp. 49–53, Jan. 2005, doi: https://doi.org/10.1016/j.apergo.2004.09.004.

[8] R. C. Browning, J. R. Modica, R. Kram, and A. Goswami, "The Effects of Adding Mass to the Legs on the Energetics and Biomechanics of Walking," *Medicine & Science in Sports & Exercise*, vol. 39, no. 3, pp. 515–525, Mar. 2007, doi: https://doi.org/10.1249/mss.0b013e31802b3562.

[9] T. W. Dorn, J. M. Wang, J. L. Hicks, and S. L. Delp, "Predictive Simulation Generates Human Adaptations during Loaded and Inclined Walking," *PLOS ONE*, vol. 10, no. 4, p. e0121407, Apr. 2015, doi: https://doi.org/10.1371/journal.pone.0121407.

[10] A. Seth et al., "OpenSim: Simulating musculoskeletal dynamics and neuromuscular control to study human and animal movement," *PLOS Computational Biology*, vol. 14, no. 7, p. e1006223, Jul. 2018, doi: https://doi.org/10.1371/journal.pcbi.1006223.

[11] T. Geijtenbeek, The Hyfydy Simulation Software, 2021, https://hyfydy.com

[12] T. Geijtenbeek, "SCONE: Open Source Software for Predictive Simulation of Biological Motion," *Journal of Open Source Software*, vol. 4, no. 38, p. 1421, Jun. 2019, doi: https://doi.org/10.21105/joss.01421.

[13] Y. Han, F. C. Sup, Z. Han, and Z. Mi, "Effects of Added Mass on Muscle Activity and Joint Movement During Walking," *Journal of bionic engineering/Journal of Bionics Engineering*, vol. 20, no. 6, pp. 2703–2715, Aug. 2023, https://doi.org/10.1007/s42235-023-00417-y.

[14] J. P. Charles, B. Grant, K. D'Août, and K. T. Bates, "Subject-specific muscle properties from diffusion tensor imaging significantly improve the accuracy of musculoskeletal models," *Journal of Anatomy*, vol. 237, no. 5, pp. 941–959, Jun. 2020, doi: https://doi.org/10.1111/joa.13261.

[15] T. Piazza, Johan Lundström, A. Kunz, and M. Fjeld, "Predicting Missing Markers in Real-Time Optical Motion Capture," *Lecture notes in computer science*, pp. 125–136, Jan. 2009, doi: https://doi.org/10.1007/978-3-642-10470-1_11.

[16] Movella, "Xsens MVN link", *Movella.com* https://www.movella.com/products/motion-capture/xsens-mvn-link

[17] M. P. Mavor, G. B. Ross, A. L. Clouthier, T. Karakolis, and R. B. Graham, "Validation of an IMU Suit for Military-Based Tasks," *Sensors*, vol. 20, no. 15, p. 4280, Jan. 2020, doi: https://doi.org/10.3390/s20154280.

[18] N. Hansen, "The CMA evolution strategy: a comparing review", *Towards a New Evolutionary Computation*, pp. 75–102, 2006

[19] K. H. Hunt and F. R. E. Crossley, "Coefficient of Restitution Interpreted as Damping in Vibroimpact," *Journal of Applied Mechanics*, vol. 42, no. 2, pp. 440–445, Jun. 1975, doi: https://doi.org/10.1115/1.3423596.

[20] H. Geyer and H. Herr, "A Muscle-Reflex Model That Encodes Principles of Legged Mechanics Produces Human Walking Dynamics and Muscle Activities," *IEEE Transactions on Neural Systems and Rehabilitation Engineering*, vol. 18, no. 3, pp. 263–273, Jun. 2010, doi: https://doi.org/10.1109/tnsre.2010.2047592.

[21] J. M. Wang, S. R. Hamner, S. L. Delp, and V. Koltun, "Optimizing locomotion controllers using biologically-based actuators and objectives," *ACM Transactions on Graphics*, vol. 31, no. 4, pp. 1–11, Aug. 2012, doi: https://doi.org/10.1145/2185520.2185521.

[22] K. Veerkamp et al., "Evaluating cost function criteria in predicting healthy gait," *Journal of Biomechanics*, vol. 123, p. 110530, Jun. 2021, doi: https://doi.org/10.1016/j.jbiomech.2021.110530.

[23] T. Pozzo, A. Berthoz, and L. Lefort, "Head stabilization during various locomotor tasks in humans," *Experimental Brain Research*, vol. 82, no. 1, Aug. 1990, doi: https://doi.org/10.1007/bf00230842.

[24] F.C. Anderson, "A dynamic optimization solution for a complete cycle of normal gait". *PhD thesis* , University of Texas at Austin, 1999

[25] L. J. Bhargava, M. G. Pandy, and F. C. Anderson, "A phenomenological model for estimating metabolic energy consumption in muscle contraction," *Journal of Biomechanics*, vol. 37, no. 1, pp. 81–88, Jan. 2004, doi: https://doi.org/10.1016/s0021-9290(03)00239-2.

[26] A. Rajagopal, C. L. Dembia, M. S. DeMers, D. D. Delp, J. L. Hicks, and S. L. Delp, "Full-Body Musculoskeletal Model for Muscle-Driven Simulation of Human Gait," *IEEE Transactions on Biomedical Engineering*, vol. 63, no. 10, pp. 2068–2079, Oct. 2016, doi: https://doi.org/10.1109/tbme.2016.2586891.

[27] M. Millard, T. Uchida, A. Seth, and S. L. Delp, "Flexing Computational Muscle: Modeling and Simulation of Musculotendon Dynamics," *Journal of Biomechanical Engineering*, vol. 135, no. 2, Feb. 2013, doi: https://doi.org/10.1115/1.4023390.

[28] D. G. Thelen and F. C. Anderson, "Using computed muscle control to generate forward dynamic simulations of human walking from experimental data," *Journal of Biomechanics*, vol. 39, no. 6, pp. 1107–1115, Jan. 2006, doi: https://doi.org/10.1016/j.jbiomech.2005.02.010.

[29] B. R. Umberger, "Stance and swing phase costs in human walking," *Journal of the Royal Society Interface*, vol. 7, no. 50, pp. 1329–1340, Sep. 2010, doi: https://doi.org/10.1098/rsif.2010.0084.

[30] B. R. UMBERGER, K. G. M. GERRITSEN, and P. E. MARTIN, "A Model of Human Muscle Energy Expenditure," *Computer Methods in Biomechanics and Biomedical Engineering*, vol. 6, no. 2, pp. 99–111, May 2003, doi: https://doi.org/10.1080/1025584031000091678.

[31] T. K. Uchida, J. L. Hicks, C. L. Dembia, and S. L. Delp, "Stretching Your Energetic Budget: How Tendon Compliance Affects the Metabolic Cost of Running," *PLOS ONE*, vol. 11, no. 3, p. e0150378, Mar. 2016, doi: https://doi.org/10.1371/journal.pone.0150378.

[32] C. L. Dembia, A. Silder, T. K. Uchida, J. L. Hicks, and S. L. Delp, "Simulating ideal assistive devices to reduce the metabolic cost of walking with heavy loads," *PLOS ONE*, vol. 12, no. 7, p. e0180320, Jul. 2017, doi: https://doi.org/10.1371/journal.pone.0180320.

[33] L. N. Jessup, L. A. Kelly, A. G. Cresswell, and G. A. Lichtwark, "Validation of a musculoskeletal model for simulating muscle mechanics and energetics during diverse human hopping tasks," *Royal Society open science*, vol. 10, no. 10, Oct. 2023, doi: https://doi.org/10.1098/rsos.230393.

[34] C. M. O'Connor, S. K. Thorpe, M. J. O'Malley, and C. L. Vaughan, "Automatic detection of gait events using kinematic data," *Gait & Posture*, vol. 25, no. 3, pp. 469–474, Mar. 2007, doi: https://doi.org/10.1016/j.gaitpost.2006.05.016.

[35] S. Nolte, R. Rein, and Oliver Jan Quittmann, "Data Processing Strategies to Determine Maximum Oxygen Uptake: A Systematic Scoping Review and Experimental Comparison with Guidelines for Reporting," *Sports medicine* , vol. 53, no. 12, pp. 2463–2475, Aug. 2023, doi: https://doi.org/10.1007/s40279-023-01903-3.

[36] J.M. Brockway, "Derivation of formulae used to calculate energy expenditure in man", *Human nutrition. Clinical Nutrition* , vol 41, pp. 463–471. 1987

[37] D. Debertin, A. Wargel, and M. Mohr, "Reliability of Xsens IMU-Based Lower Extremity Joint Angles during In-Field Running," *Sensors*, vol. 24, no. 3, p. 871, Jan. 2024, doi: https://doi.org/10.3390/s24030871.

[38] A. D. Koelewijn, D. Heinrich, and A. J. van den Bogert, "Metabolic cost calculations of gait using musculoskeletal energy models, a

comparison study," PLOS ONE, vol. 14, no. 9, p. e0222037, Sep. 2019, doi: https://doi.org/10.1371/journal.pone.0222037.

[39] I. Coifman, R. Kram, and R. Riemer, "Joint kinematic and kinetic responses to added mass on the lower extremities during running," Applied Ergonomics, vol. 114, pp. 104050–104050, Jan. 2024, doi: https://doi.org/10.1016/j.apergo.2023.104050.

[40] C. Devroey, I. Jonkers, A. de Becker, G. Lenaerts, and A. Spaepen, "Evaluation of the effect of backpack load and position during standing and walking using biomechanical, physiological and subjective measures," *Ergonomics*, vol. 50, no. 5, pp. 728–742, May 2007, doi: https://doi.org/10.1080/00140130701194850.

[41] V. Camomilla, R. Dumas, and A. Cappozzo, "Human movement analysis: The soft tissue artefact issue," *Journal of Biomechanics*, vol. 62, pp. 1–4, Sep. 2017, doi: https://doi.org/10.1016/j.jbiomech.2017.09.001.

[42] W. H. K. de Vries, H. E. J. Veeger, C. T. M. Baten, and F. C. T. van der Helm, "Magnetic distortion in motion labs, implications for validating inertial magnetic sensors," *Gait & Posture*, vol. 29, no. 4, pp. 535–541, Jun. 2009, doi: https://doi.org/10.1016/j.gaitpost.2008.12.004.

[43] A. B. Arsenault, D. A. Winter, and R. G. Marteniuk, "Is there a 'normal' profile of EMG activity in gait?," *Medical & Biological Engineering & Computing*, vol. 24, no. 4, pp. 337–343, Jul. 1986, doi: https://doi.org/10.1007/bf02442685.

[44] J. Wenghofer, Kristen HE Beange, W. C. Ramos, M. P. Mavor, and R. B. Graham, "Dynamic assessment of spine movement patterns using an RGB-D camera and deep learning," *Journal of Biomechanics*, pp. 112012–112012, Feb. 2024, doi: https://doi.org/10.1016/j.jbiomech.2024.112012.

[45] I. Coll, "Validation of markerless motion capture for the assesment of soldier movement patters under varying body-borne loads", *MSc thesis*, available at: https://ruor.uottawa.ca/items/d35803c9-b957-416e-8395-4b267569c400

Indirect calorimetry data
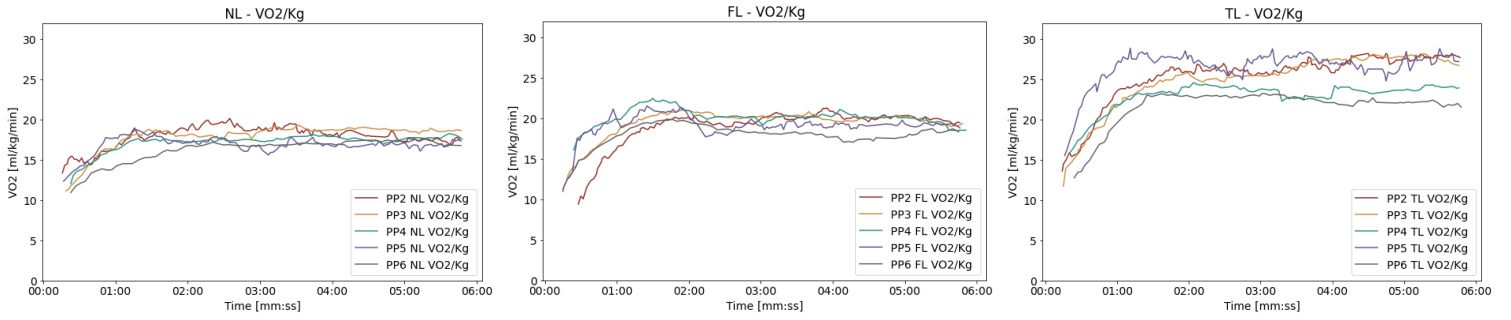
VO2 uptake per kg body mass of all test subjects and load conditions
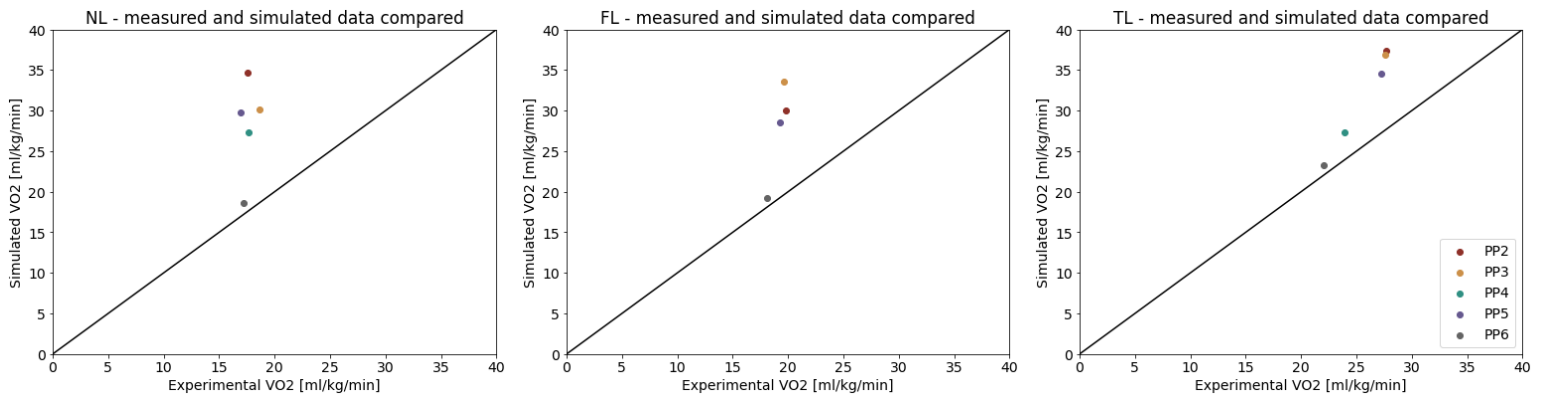
Simulated VO2 umptake compared to measured VO2 of all subjects in all load conditions

Kinematic and GRF trend Visualisation

Analysis of trends between load conditions within measured results compared to those within simulated result. Angle differences are in degrees, time differences are in % of gait cycle. (*) indicates significant difference from Unloaded, (+) indicates significant difference from other load condition
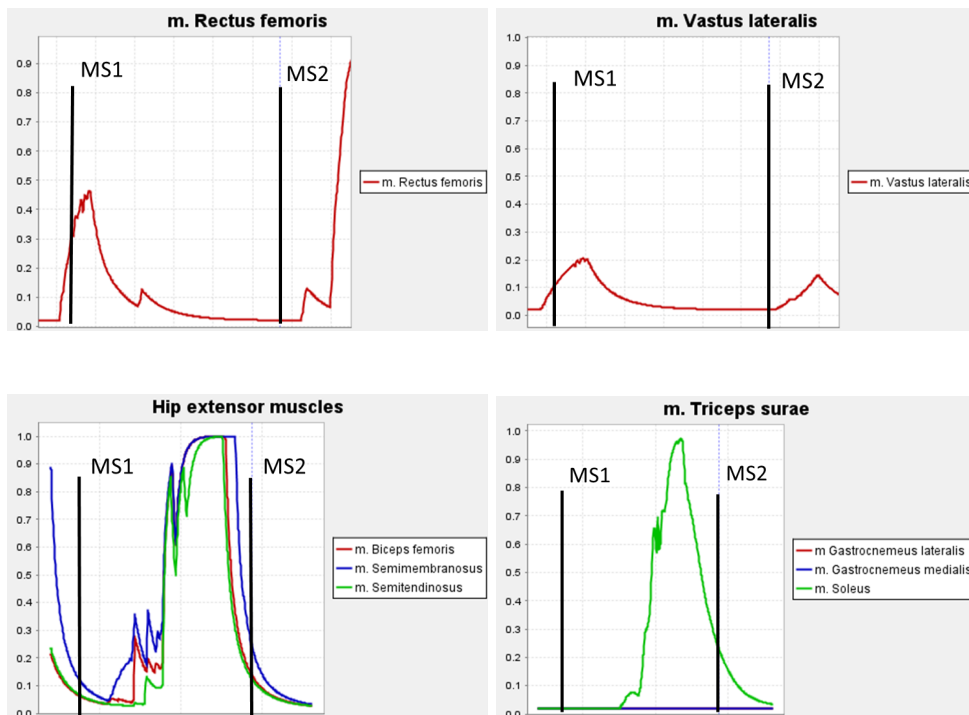
Frontal ground reaction forces

Vertical ground reaction forces
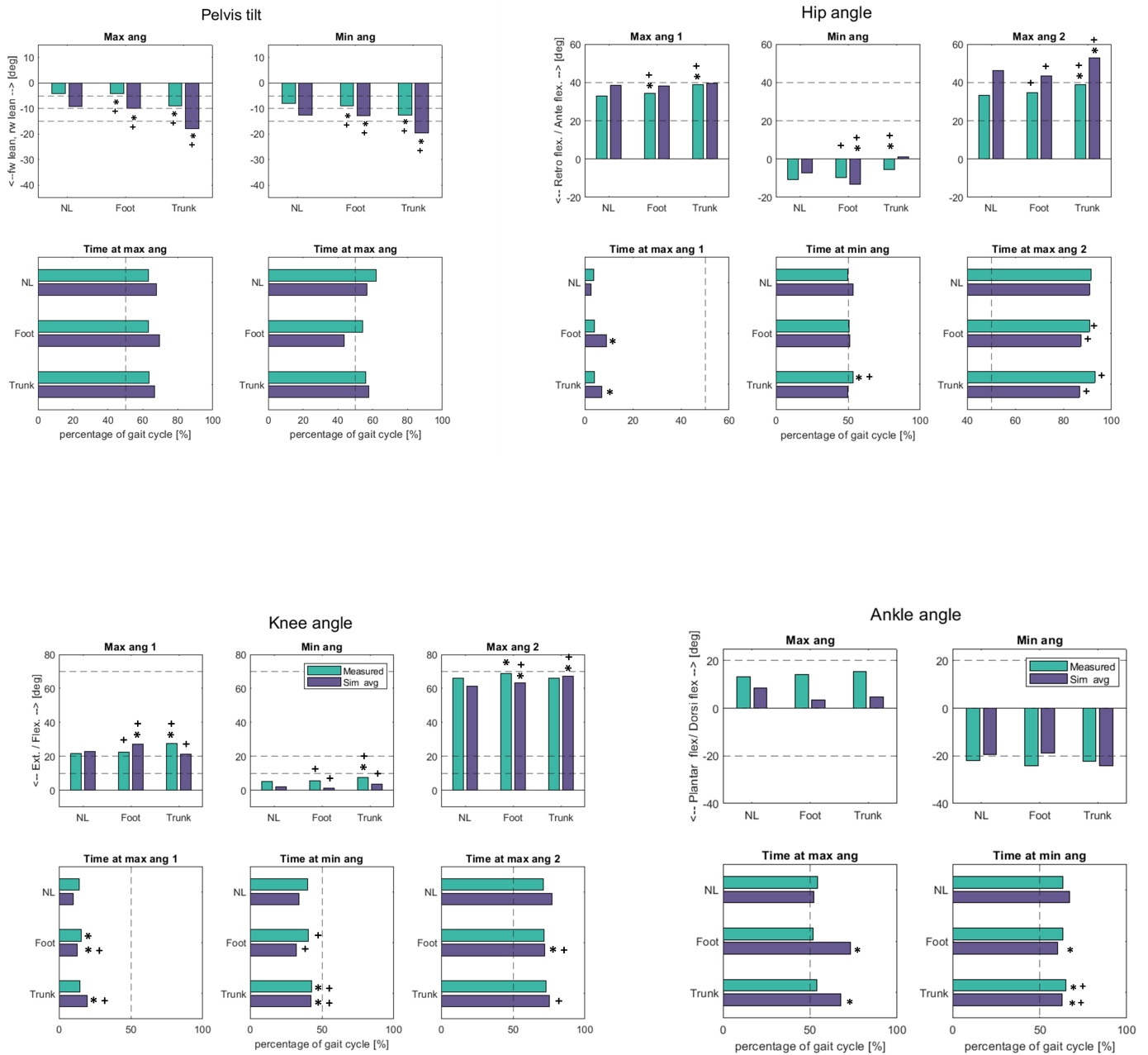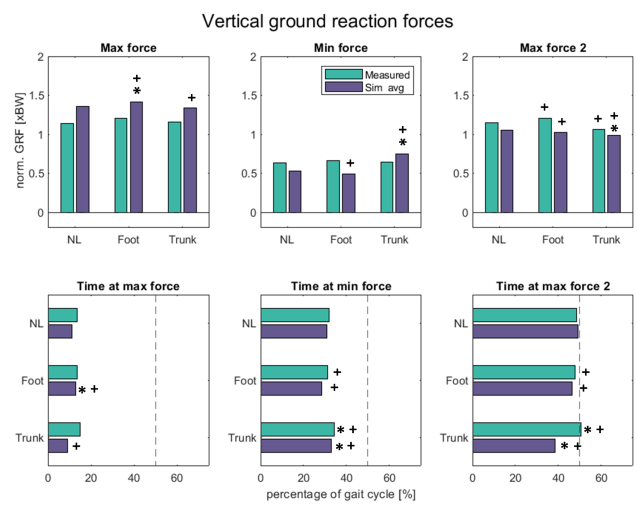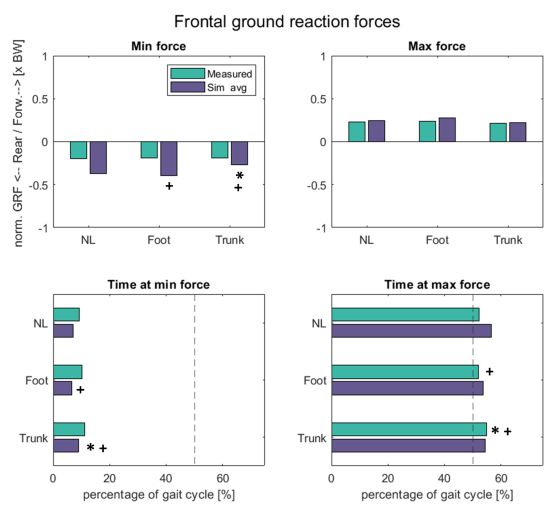
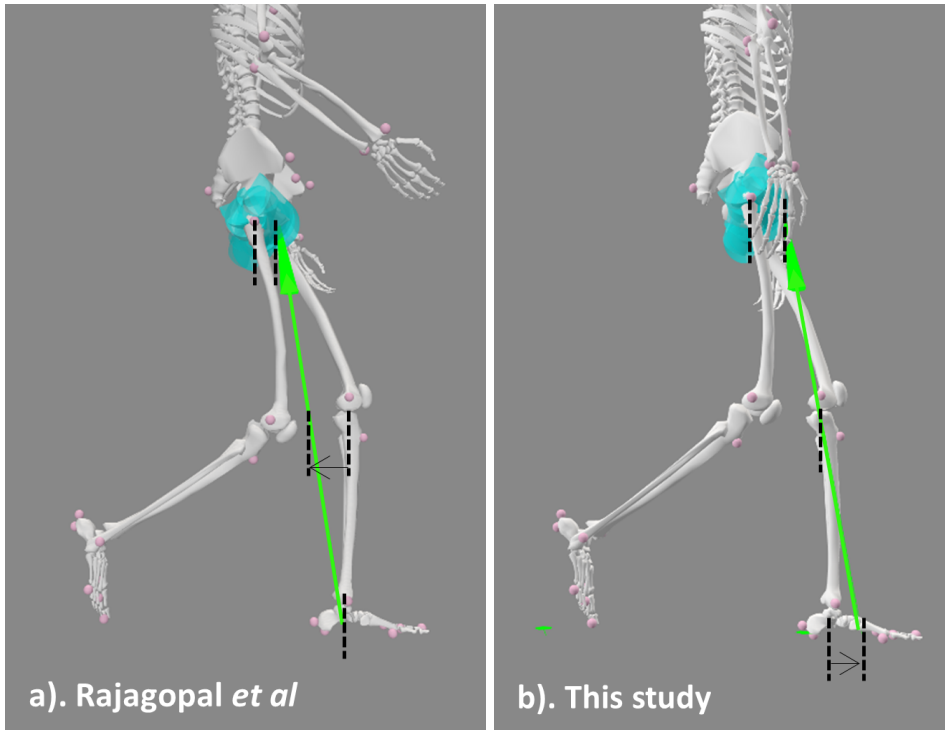*C-1: Muscle activation comparison*
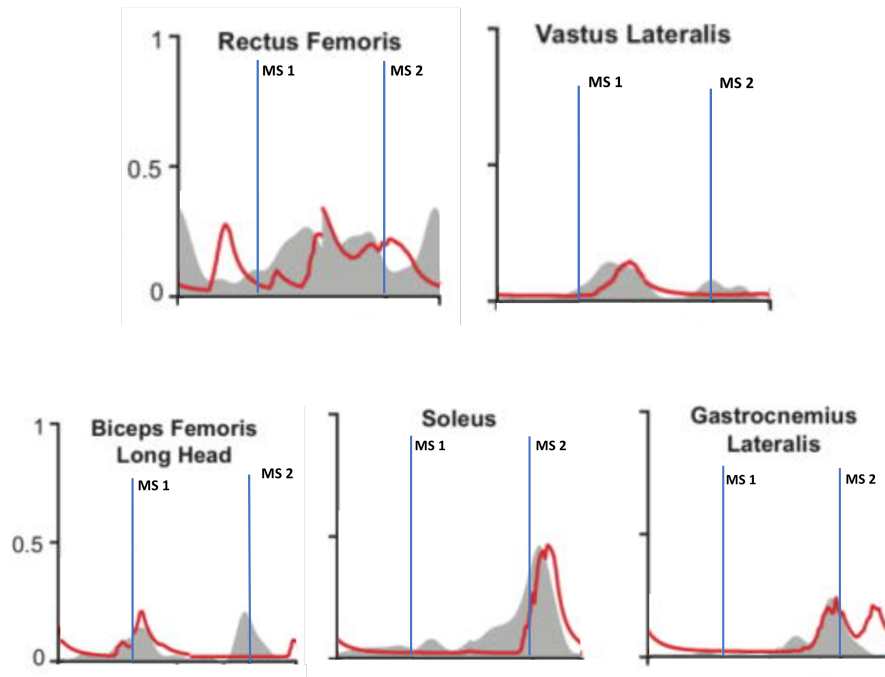
Normal gait EMG (shaded gray) and simulated large muscle activity, adapted from Ragagopal et al [26]

Unloaded gait muscle activation of a typical simulation of this study.

GRF vector comparison at toe-off of the right leg. Black dashed lines and arrows indicate differences in vector moment arms w.r.t. joints rotation centres